THE JOURNAL OF PHYSICAL CHEMISTRY C

ARTICLE

pubs.acs.org/JPCC

First-Principles Study of H^+ Intercalation in Layer-Structured $LiCoO_2$

Xiao Gu,[*,†] Jin-long Liu,[‡] Ji-hui Yang,[§] Hong-jun Xiang,[§] Xin-gao Gong,[*,§] and Yong-yao Xia[*,‡]

[†]Lab for Computational Physical Sciences (MOE), Department of Environmental Sciences and Engineering, Fudan University, Shanghai 200433, China

[‡]Department of Chemistry, Shanghai Key Laboratory of Molecular Catalysis and Innovative Materials, Institute of New Energy, Fudan University, Shanghai 200433, China

[§]Lab for Computational Physical Sciences (MOE), Department of Physics, Fudan University, Shanghai 200433, China

ABSTRACT: The electrochemical stability of layer-structured $LiCoO_2$ in a Li^+-containing aqueous electrolyte solution is critically dependent on the solution pH. The capacity fades upon cycling in electrolyte solutions below pH 11. We have investigated the detailed atomic-scale mechanism of the failure of $LiCoO_2$ in the presence of H^+ using first-principles methods. In layer-structured $LiCoO_2$, lithium ion diffusion paths are two-dimensional channels between the cobalt−oxygen layers. However, in an aqueous electrolyte solution containing a considerable number of H^+ ions, H^+ will be transported into the cathodes to replace the Li^+ ions. Our calculations show that once the H^+ ions are intercalated into the Li_xCoO_2 cathode, they may covalently bond to the oxygen ions, thereby decreasing the capacity of the cathodes. We have also found that such hydrogen intercalation increases barriers to the diffusion of lithium ions. Therefore, the channels would be blocked after a sufficient number of H^+ ions have intercalated, typically after a few cycles.

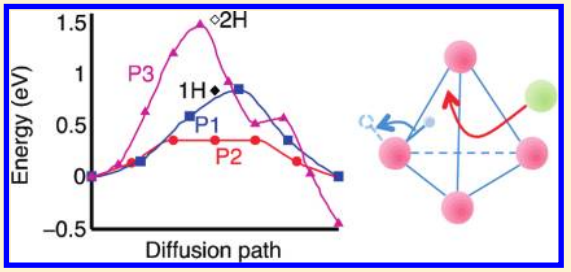

INTRODUCTION

Layer-structured $LiCoO_2$ was the first material to be used as the cathode in commercial lithium ion batteries (LIB) for the portable electronic devices market (including such devices as cell phones and laptops).[1] Transition metal oxide based cathodes have been the subjects of various efforts to improve the performance of rechargeable lithium ion batteries.[2] However, most of the research focused on systems with nonaqueous electrolytes. Such systems are proven applications in real world, but are expensive to manufacture. Further, conductivity issues have restricted the size of available LIBs. Aqueous electrolytes represent a promising avenue for addressing these problems. In 1994, Dahn et al. reported an aqueous LIB in which VO_2 was used as the anode and $LiMn_2O_4$ was used as the cathode.[3] Unfortunately, the battery had a poor cycle life. Since then, the electrochemistry of compounds in aqueous electrolyte systems has attracted increasing attention. Only recently, the cycling stability was greatly improved.[4] We have previously shown that the electrochemical stability of the layer-structured $LiCo_{1/3}Ni_{1/3}Mn_{1/3}O_2$ and $LiCoO_2$ is critically dependent upon the system pH. In low-pH electrolyte solutions, these structures were unstable and lost capacity upon cycling.[5] The critical factor differentiating the behavior of nonaqueous and the aqueous electrolytes is the action of the H^+. Because H^+ occupy much less volume than other cations, they may be more chemically active. Electrochemical studies demonstrated that H^+ intercalation during the discharge process results in large electrode polarization, leading to capacity fading.[6] Infrared spectroscopy studies also confirmed the existence of H^+ in the layer-structured cathodes during delithiation.[7]

It is valuable to understand how these materials gradually become dysfunctional after multiple cycles, prolonged storage or under other conditions. Defects introduced from many possible sources could play important roles in the fading of the active materials. In this work, we analyzed the detailed atomic-scale mechanism of capacity fading of $LiCoO_2$ upon cycling in the presence of hydrogen using first-principles methods.

THEORETICAL METHOD

To explore the failure mechanism of $LiCoO_2$ at the atomic scale, we employed first-principles calculations based on density functional theory (DFT). The general gradient approximation (GGA) of Perdew and Wang (PW91) was employed for the exchange-correlation functional.[8] The projector augmented wave (PAW) method was used to describe the interactions between valence electrons and the ionic cores.[9] The wave functions were expanded in a plane wave basis truncated at a plane wave energy of 450 eV. A $4 \times 4 \times 4$ Monkhorst−Pack grid was used for *k*-space sampling in the calculations. Geometry optimizations were converged to a force cutoff of 0.01 eV/Å. The nudged elastic band (NEB) method, implemented for use with DFT in the Vienna Ab-initio Simulation Package (VASP),[10,11] was employed to identify the minimum energy paths (MEP) for diffusion.

Received: March 11, 2011
Revised: May 6, 2011
Published: June 03, 2011

dx.doi.org/10.1021/jp202846p | *J. Phys. Chem. C* 2011, 115, 12672–12676

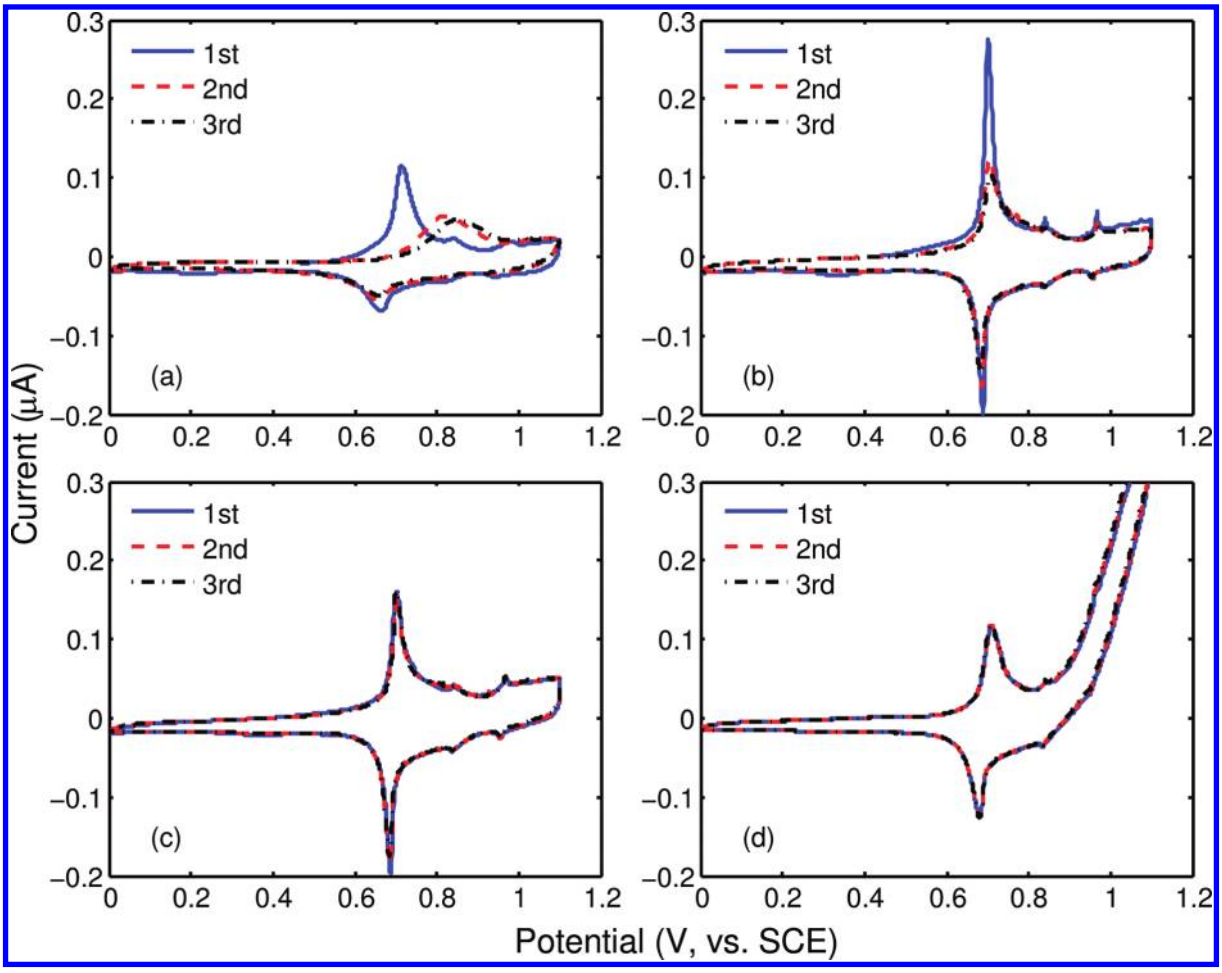

Figure 1. Cyclic voltammograms of $LiCoO_2$ in 1 mol/L Li_2SO_4 aqueous solution, with a scan rate of 10 mV/s and voltages from 0 to 1.1 V vs the saturated calomel electrode (SCE). Different H^+ concentrations were investigated, with pH values of (a) pH 7, (b) pH 9, (c) pH 11, and (d) pH 13.

RESULTS AND DISCUSSION

The electrochemical stability of $LiCoO_2$ cycling is investigated using the powder microelectrode technique. Figure 1 shows the cyclic voltammograms (CV) of $LiCoO_2$ in aqueous electrolyte solutions with several pH values (7, 9, 11, and 13). These voltammograms show that the electrochemical stability of $LiCoO_2$ is critically dependent on the electrolyte pH. Below pH 9, $LiCoO_2$ is not electrochemically stable, and its stability increases with the pH of the solution. $LiCoO_2$ becomes stable at pH 11, as shown in Figure 1c. These results suggest that the stability of $LiCoO_2$ in the aqueous electrolyte solution is solely dependent on the pH (i.e., the H^+ concentration) of the solution. The chemical instability in the low-pH electrolyte solutions may be due to intercalation of H^+.

Layer-structured $LiCoO_2$ has a rhomboid structure with a-b-c layers. The primitive cell of $LiCoO_2$ contains one lithium ion, one cobalt ion and two oxygen ions, as shown in Figure 2(a). We constructed a super cell by expanding the primitive cell to *S*7, with a volume seven times that of the primitive cell. Shown in Figure 2c, a slice of 7 lithium ions was placed in a two-dimensional plane perpendicular to the diagonal of the cell. This lithium layer represents the diffusion channel. The diffusion mechanism in many cathodes has been the subject of much investigation, both theoretical and experimental.[12−16] The activation barrier for a divacancy mechanism was found to be around 0.4 eV.[17]

The substitutional positions of the hydrogens in the $LiCoO_2$ structure are very important in understanding the detailed mechanism. It might be reasonably assumed that the hydrogens directly replace the lithium ions because both ions are small and positively charged. In layer-structured $LiCoO_2$, the lithium ion is located in the center of an octahedron of six oxygen anions. In a general center-occupied octahedron, the ratio of the radii of the anions and cations must fall in a reasonable range to keep the structure electrically stable.[18] Figure 3 illustrates an octahedron by one cations and six anions. R_a and R_c are the radii of the cations and anions, respectively. The interspace between the two anions is labeled x. In the octahedron, where $2(R_a + R_c) = \sqrt{2}(2R_a + x)$, x should always be positive to separate the anions. R_c/R_a should thus be greater than 0.414. As a six-coordinate ion in $LiCoO_2$, the lithium ion has a ratio of 0.43 with respect to the oxygen ions, a value that is slightly greater than 0.414. The radius of the hydrogen ion is much smaller, which violates the ratio threshold; thus, hydrogen cannot be stably bound in the center of the oxygen octahedron. In our calculations, the structure with hydrogen substituted into the lithium position is metastable and is easily distorted. In this case, small structural distortions would lead to the hydrogen being attracted toward one of the oxygen ions of the octahedron (Figure 4a). In fact, the hydrogen is bonded to one of the oxygen ions with a stronger oxygen−hydrogen covalent bond. The H−O bond length is about 1.0 Å,

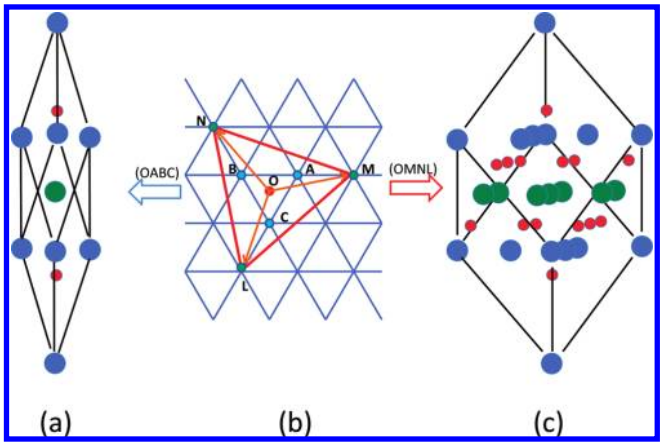

Figure 2. Primitive and supercells of the layer-structured $LiCoO_2$ cathode. The blue balls represent cobalt ions, the red balls represent oxygen ions, and the green balls represent lithium ions. (a) Primitive cell containing one cobalt ion, one lithium ion, and two oxygen ions aligned along the diagonal. (b) The honeycomb lattice of the cobalt layer. The center dot (**O**) represents the cobalt ion in the next layer. **OA**, **OB**, and **OC** are the basis vectors of the primitive cell. (c) The S7 supercell. **OM**, **ON**, and **OL** in (b) are the basis vectors for the supercell (S7).

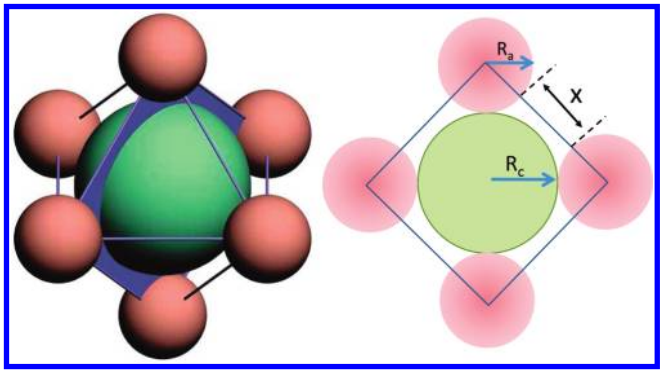

Figure 3. Left panel: illustration of an anion octahedron containing one cation in the center. Right panel: cross section of the octahedron perpendicular to one of the axes (blue plane, left). The green and red circles represent the cation and anions, respectively. The radii of the anions and cation are R_a and R_c, respectively. The distance separating the anions is labeled x.

the same as that of the water molecule, in agreement with previous results.[19,20] Additionally, the distances between the hydrogen and other oxygen ions are approximately 2.0 Å, which is close to the hydrogen bond length in liquid water. The total energy of the system is 2.0 eV lower than that of center substitution at the lithium position.

Figure 4b shows the relaxed structure with two hydrogen substitutions. Both hydrogen ions are displaced from the original lithium positions by nearby oxygen ions. In this figure, both hydrogen ions are displaced on one side of the lithium. However, it is not necessary to keep them on the same side. Our calculations show that the hydrogen could also be bonded to the oxygen ions in the other layer. Because the covalent bond of H−O is 2.0 eV lower than the H−O bond on the metastable lithium site, it is not likely to extract the hydrogen into the lithium diffusion channels, where the cations have a weaker ionic bond to the oxygen.

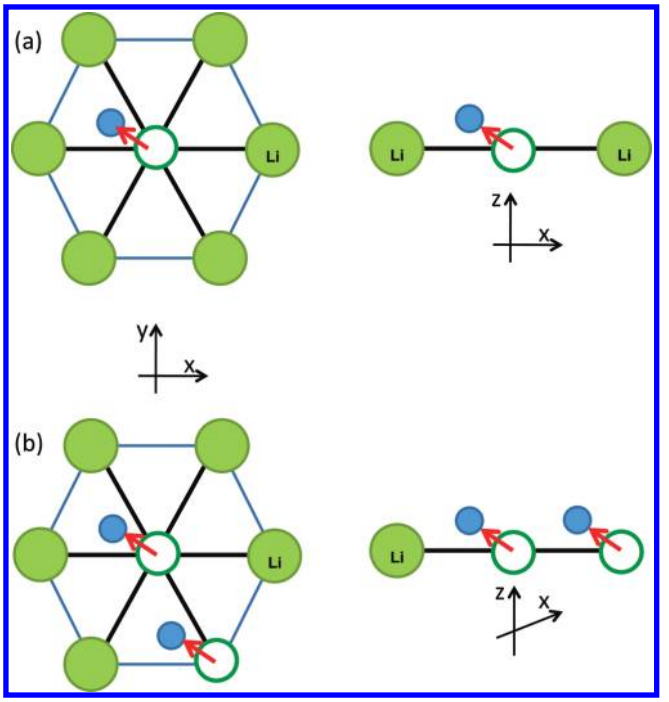

Figure 4. Substitutional hydrogens in the lithium layer. The green circles are the lithium ions, and the open circles indicate the positions of the lithium vacancies. (a) One substitutional hydrogen in the lithium layer. Left panel, top view; right panel, side view. The hydrogen is attracted by one of the nearby oxygen ions. (b) The case with two substitutional hydrogens.

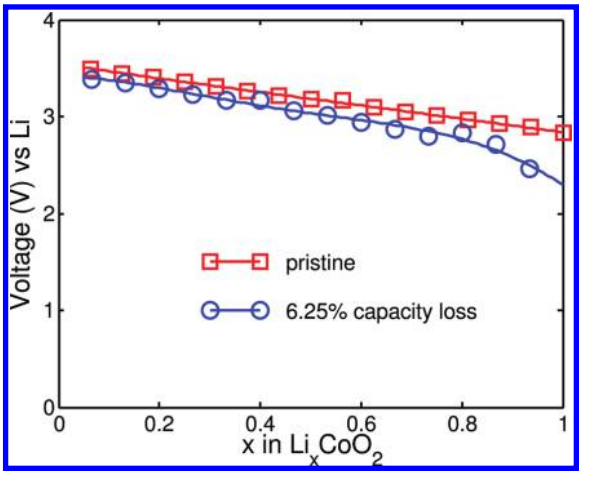

Figure 5. Comparison of the discharge voltages of pristine $LiCoO_2$ and $LiCoO_2$ with 6.25% capacity loss caused by intercalated hydrogen. The potential V (relative to lithium metal) is calculated by $V = (E_{Li_xCoO_2} + (1-x)E_{Li(metal)} - E_{LiCoO_2})/((1-x)F)$.

Figure 5 shows the discharging of a pristine $LiCoO_2$ and a H-intercalated $LiCoO_2$. To minimize the size effect, a larger supercell containing 16 lithium atoms is employed. This supercell is generated by extending S7 in Figure 2. In this cell, when one of lithiums is substituted by hydrogen, it is corresponding to 6.25% capacity loss. Both of the potentials of the cathodes decrease as the number of intercalated lithium ions increases. However, the presence of hydrogen significantly lowers the working voltage of the H-intercalated cathode at the end of the

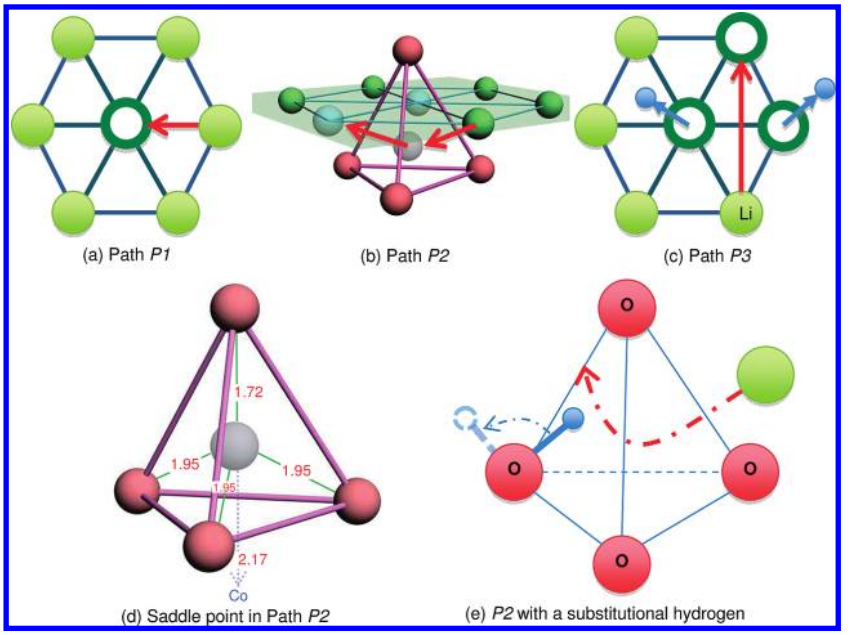

Figure 6. Diffusion paths of the lithium ions. The green balls represent lithium ions, open balls indicate the positions of lithium vacancies, red balls represent oxygen ions, and arrows show the directions of diffusion. (a) Direct diffusion, path P1: the lithium ion diffuses directly to its nearest neighbor. (b) Diffusion path P2: a divacancy is formed by two adjacent vacancies (lighter balls). The gray ball is the intermediate state in this path. (c) Diffusion path P3: substitutional hydrogens occupy two nearest neighbors. The diffusing lithium goes over the hydrogens to the second nearest neighbor. (d) The saddle point in path P2. (e) Divacancy path with substitutional hydrogen.

discharging as the hydrogens are more crowded by the intercalated lithium ions. It is believed that most of the energy loss is to the result of hydrogen−oxygen bonds. We have also calculated the formation energy of defects formed by the presence of substitutional hydrogen with a few lithium vacancies nearby. The formation energy of such defect $E_F(N)$ is defined as $E_N - E_N^H$, where E_N is the total energy with N lithium vacancies and E_N^H is the energy including the substitutional hydrogen. $E_F(N)$ increases with the number of the vacancies. To further confirm this effect, we have compared different configurations of the vacancies with hydrogens and found that the total energy of two vacancies locating nearby the hydrogen atom is 0.32 eV lower than that of the vacancies are away from the hydrogen. This differential becomes 0.37 eV in the three vacancies case. This means that it is energetically favorable for the hydrogen to be located next to vacancies; i.e., once the hydrogen is intercalated into the structure, lithium ions are not willing to be intercalated nearby.

We next investigated the diffusion mechanisms for both single vacancy and divacancy.[17] Figure 6a shows the direct diffusion of a lithium ion. The vacancy is located in the center, with six nearest neighbors. The diffusion path is defined as one of these neighbors into the vacancy. This diffusion path, labeled P1, associates with only one vacancy. Although this diffusion is a nearest-neighbor process, the diffusing lithium ion has to push the cobalt−oxygen layers, which results in a higher barrier. The barrier is calculated to be 0.80 eV for this direct single-vacancy diffusion. Figure 6b shows the path with two adjacent vacancies (P2). This path is defined as the nearest lithium curved path, which passes through the center of the tetrahedron of the four oxygen ions (red balls). Because there are two vacancies, such a path would not displace lithium near the tetrahedron. In fact, with the second lithium absent, the barrier for diffusion into the other vacancy is reduced to 0.37 eV. Figure 6d shows the saddle point of path P2, which is

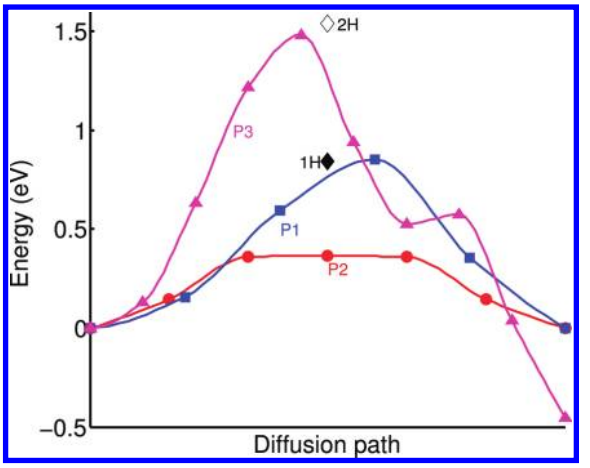

Figure 7. Diffusion barriers of paths P1, P2, and P3. Path P1, the direct single-vacancy hopping path, has a barrier of 0.80 eV. Path P2, the divacancy path, has a lower barrier, 0.37 eV. In path P3, there are two hydrogens in the diffusion path (representing a high concentration of hydrogen substitution), resulting in a much higher barrier, 1.50 eV. The static calculations for the saddle point in P2 with 1 and 2 hydrogens nearby are shown as the black and open diamonds, respectively. The involvement of the hydrogens in the path would increase the barrier significantly.

located on the center of the oxygen ion tetrahedron. The tetrahedron is located directly above a cobalt ion. The lithium ion is displaced to the top oxygen because of the repulsion from the Co^{3+} ion.

Figure 6e shows the diffusing lithium ion passing across the center of the oxygen tetrahedron, while one of the oxygen ions hosts the substitutional hydrogen. Initially, the hydrogen−oxygen bond could be oriented either outward or inward. If the

bond is oriented inward, once the diffusing lithium ion is within the tetrahedron, it will drive the hydrogen outward. However, the saddle point in P2 will have disappeared due to the repulsion from the hydrogen. A static calculation with the diffusing lithium ion fixed at the saddle point in P2 yielded a total energy of 0.80 eV above that of the beginning of the path, shown as the black diamond in Figure 7. This result indicates that the divacancy path is no longer preferred. To understand the influence of additional substitutional hydrogens, we modeled a case in which the diffusing lithium ion must push two adjacent hydrogens. This case, shown in Figure 6c, involves two substitutional hydrogens in the path of the diffusing lithium ion, which are attracted to the oxygen ions and slightly displaced from their original substitutional sites. In this path, labeled P3, the lithium moves to the vacancy in its second nearest neighbor.

Figure 7 shows the diffusion barriers for all paths. The red circles represent the divacancy mechanism, with a barrier of 0.37 eV (P2). The blue squares represent direct diffusion, with a barrier 0.80 eV (P1). The black diamonds represent the relative energies of the static calculation for the saddle point in P2 with substitutional hydrogen. The open diamonds represent the case with two nearby hydrogen ions. The violet triangles represent the path with two hydrogens (P3). In path P3, NEB predicted a diffusion barrier of 1.50 eV, a barrier higher than those of both P1 and P2.

CONCLUSION

In conclusion, we investigated the electrochemical profile of layer-structured $LiCoO_2$ in aqueous electrolyte solution. We found that the electrochemical stability of the $LiCoO_2$ is critically dependent on the H^+ concentration. $LiCoO_2$ is not electrochemically stable in electrolyte solutions with pH values less than 9, but it becomes stable with pH values above 11. Our first-principles study showed that the substitutional hydrogen ions are bonded to the oxygen atoms via H−O bonds, displacing the hydrogen atoms from the centers of the oxygen octahedrons. Hydrogens are more likely to stay near the vacancies. The formation energies of the vacancy−hydrogen complex defects increase with the number of the vacancies. By the presence of the hydrogen, the working voltages of the contaminated cathodes will be reduced at the end of the discharging. Furthermore, the divacancy diffusion channels for the lithium ions will also be blocked by the increased diffusion barriers. A small number of the intercalated hydrogens will not significantly affect the performance of the cathodes. However, as increasing numbers of hydrogens are involved in repeated charging and discharging cycles, the area of the cathode containing intercalated hydrogens will increase. Once these hydrogens are aligned, the diffusion barrier for the lithium ions will become several times higher. This increase in the barrier will block the diffusion channels for the lithium ions.

AUTHOR INFORMATION

Corresponding Author

*E-mail: gx@fudan.edu.cn (X.G.); xggong@fudan.edu.cn (X.-g. G.); yyxia@fudan.edu.cn (Y.-y.X.).

ACKNOWLEDGMENT

This work was partially supported by the National Natural Science Foundation of China and the Shanghai Science & Technology Committee.

REFERENCES

(1) Armstrong, A. R.; Bruce, P. G. *Nature* **1996**, *381*, 499–500.
(2) Whittingham, M. S. *Chem. Rev.* **2004**, *104*, 4271–4302.
(3) Li, W.; Mckinnon, W. R.; Dahn, J. R. *J. Electrochem. Soc.* **1994**, *141*, 2310–2316.
(4) Luo, J. Y.; Cui, W. J.; He, P.; Xia, Y. Y. *Nat. Chem.* **2010**, *2*, 760–765.
(5) Wang, Y. G.; Lou, J. Y.; Wu, W.; Wang, C. X.; Xia, Y. Y. *J. Electrochem. Soc.* **2007**, *154*, A228–A234.
(6) Zheng, J.; Chen, J. J.; Jia, X.; Song, J.; Wang, C.; Zheng, M. S.; Dong, Q. F. *J. Electrochem. Soc.* **2010**, *157*, A702–A706.
(7) Venkatraman, S.; Manthiram, A. *J. Solid State Chem.* **2004**, *177*, 4244–4250.
(8) Perdew, J. P.; Wang, Y. *Phys. Rev. B* **1992**, *45*, 13244–13249.
(9) Perdew, J. P.; Chevary, J. A.; Vosko, S. H.; Jackson, K. A.; Pederson, M. R.; Singh, D. J.; Fiolhais, C. *Phys. Rev. B* **1992**, *46*, 6671–6687.
(10) Kresse, G.; Furthmuller, J. *Phys. Rev. B* **1996**, *54*, 11169–11186.
(11) Henkelman, G.; Jonsson, H. *J. Chem. Phys.* **2000**, *113*, 9978–9985.
(12) Kang, K.; Ceder, G. *Phys. Rev. B* **2006**, *74*, 094105.
(13) Van der Ven, A.; Ceder, G. *Electrochem. Solid-State Lett.* **2000**, *3*, 301–304.
(14) Xu, B.; Meng, S. *J. Power Sources* **2010**, *195*, 4971–4976.
(15) Wen, S. H.; Hou, Z. F.; Han, K. L. *J. Phys. Chem. C* **2009**, *113*, 18436–18440.
(16) Wilkening, M.; Lyness, C.; Armstrong, A. R.; Bruce, P. G. *J. Phys. Chem. C* **2009**, *113*, 4741–4744.
(17) Van der Ven, A.; Ceder, G. *J. Power Sources* **2001**, *97−98*, 529–531.
(18) Kellerman, D. G.; Gabuda, S. P.; Zhuravlev, N. A.; Semenova, A. S.; Denisova, T. A.; Pletnev, R. N. *J. Struct. Chem.* **2007**, *48*, 462–466.
(19) Fang, C. M.; de Wijs, G. A. *Chem. Mater.* **2006**, *18*, 1169–1173.
(20) Benedek, R.; Thackeray, M. M.; van de Walle, A. *Chem. Mater.* **2008**, *20*, 5485–5490.